The role of submarine landslides in the initiation and evolution of moat-drift contourite systems

YUXIANG YANG [a, c, f], WEI LI [a, b]*, TIAGO M. ALVES [d], SONG JING [b]*, MICHELE REBESCO [e] and JIN YANG [f, g]

[a] National Engineering Research Center of Gas Hydrate Exploration and Development, Guangzhou Marine Geological Survey, China Geological Survey, Guangzhou, Guangdong 511458, China

[b] Laboratory of Ocean and Marginal Sea Geology, South China Sea Institute of Oceanology, Chinese Academy of Sciences, Guangzhou 510301, China

[c] School of Resources and Environment, Henan Polytechnic University, Jiaozuo, 454003, China

[d] 3D Seismic Lab, School of Earth and Environmental Sciences, Cardiff University, Main Building, Park Place, Cardiff, CF10 3AT, United Kingdom

[e] Istituto Nazionale di Oceanografiae di Geofisica Sperimentale (OGS), Borgo Grotta Gigante 42/C, Sgonico, 34010 Trieste, Italy

[f] College of Safety and Ocean Engineering, China University of Petroleum-Beijing, Beijing, 102249, China

[g] China National Offshore Oil Corporation South China Sea Oil & Gas Energy Academician Workstation, Haikou 570312, China

Correspondence to: Dr. Wei Li (wli@scsio.ac.cn) and Dr. Song Jing (jingsong@scsio.ac.cn)

ABSTRACT

Moat-drift contourite systems, formed by interaction of alongslope bottom currents with bathymetric features, provide critical insights into paleoceanographic changes. However, the role of submarine landslides in their initiation and evolution remains poorly understood. To investigate these processes, this study utilizes multibeam bathymetric and three-dimensional seismic data from the Baiyun Slide, located in the northern South China Sea. Our findings reveal a 600-m-wide, 50-m-deep moat incised along the steep escarpment of the Baiyun Slide headwall, flanked by a ~50-m-thick sediment drift. We propose that the landslide-induced escarpment acted as a bathymetric obstacle, locally intensifying bottom current velocities and promoting flow turbulence and erosion, which facilitated moat formation. In contrast, in areas distant from the escarpment, reduced current velocities allowed for deposition of resuspended sediments, forming the drift deposits that fill the slide scar. While the surrounding slope is dominated by gravity-driven downslope sedimentary processes, the landslide-generated escarpment reconfigured local depositional system, enabling the formation of a slide-controlled secondary contourite system driven by bottom currents. This system, confined within the negative topography of the slide scar, represents a spatial shift in sedimentation from a regional downslope to a localized alongslope control. As a corollary, we present a conceptual model illustrating how submarine landslides can reshape seafloor morphology to drive bottom current-induced sedimentation in otherwise gravity-dominated deep-marine environments. This study highlights slide-controlled moat-drift contourite systems as significant components of deep-water sedimentary archives, capable of recording dynamic interactions between bottom currents and seafloor topography.

Keywords: Submarine landslides; Slide scar; Bottom currents; Moat-drift contourite system; South China Sea

INTRODUCTION

Submarine continental slopes and rises are dynamic environments shaped by both downslope and alongslope sedimentary processes (Mulder *et al.*, 2009; Ogata *et al.*, 2014; Rebesco *et al.*, 2014; Miramontes *et al.*, 2019; Mosher & Boggild, 2021; Shanmugam, 2021). Gravity-driven downslope sediment transport is primarily manifested as submarine landslides and turbidity currents (Lintern *et al.*, 2016; Wang *et al.*, 2018; Heerema *et al.*, 2020; Li *et al.*, 2020). These phenomena are capable of transporting vast volumes of sediment over long distances from the continental shelf and upper slope into deep-water environments (Smoot & King, 1993; McAdoo *et al.*, 2000; Hutton & Syvitski, 2004; ten Brink *et al.*, 2009). They significantly modify seafloor morphology and influence subsequent sedimentary processes, forming a widely recognized feedback loop on most continental margins (Normandeau *et al.*, 2019; Gatter *et al.*, 2021).

Concurrently with the across-slope transport of sediment, alongslope bottom currents (or contour currents) shape the seafloor, generating distinct erosional features like moats and depositional features such as sediment drifts (Stow *et al.*, 2002; Minisini *et al.*, 2006; Rebesco *et al.*, 2014; Wang *et al.*, 2020; Liu *et al.*, 2023; Stagna *et al.*, 2023). Importantly, depositional systems associated with contour currents provide long-term, high-resolution records of paleoclimatic and paleoceanographic change (Hernández-Molina *et al.*, 2003; Van Rooij *et al.*, 2010; Ercilla *et al.*, 2016), while holding economic potential for oil and gas exploration (Rebesco *et al.*, 2014; Miramontes *et al.*, 2019).

Over the past few decades, there have been increasing interests in understanding the interaction between submarine landslides, such as evacuation scars and accumulation zones, and gravitational processes on continental margins (Ogata *et al.*, 2012; Uenzelmann-Neben *et al.*, 2017; Sun *et al.*, 2018; Yang *et al.*, 2024). These interests are driven by factors widely recognized in most offshore regions: (1) the capacity of submarine landslides to significantly reshape seafloor morphology (Laberg *et al.*, 2005; Rebesco *et al.*, 2016; Juan *et al.*, 2018); (2) their ability to initiate localized seafloor erosion and new submarine channels and canyons through slide scars capturing gravity flows (Kneller *et al.*, 2016; Qin *et al.*, 2017; Li *et al.*, 2020; Stagna *et al.*, 2023); and (3) the complex interactions between turbidity currents and mass-transport deposits (MTDs), which facilitate the accumulation of sandy sediments and potential hydrocarbon reservoir formation (Armitage *et al.*, 2009; Kneller *et al.*, 2016; Kremer *et al.*, 2018).

Despite this growing interest, the interaction between alongslope bottom currents and submarine landslides has received comparatively less attention (Fig. 1). While moat-drift contourite systems can be influenced by seafloor features such as seamounts, carbonate buildups and local troughs (Zhang *et al.*, 2016; Zhao *et al.*, 2024), the existence of landslide-related moat-drift contourite systems has rarely been documented, representing a significant gap in our understanding of their initiation and evolution.

The South China Sea serves as an idea laboratory for studying the interaction between bottom currents and seafloor topography due to its varied oceanographic processes operating at different spatial and temporal scales (Fig. 2) (Yin *et al.*, 2019). This study uses multibeam bathymetric and three-dimensional (3D) seismic data to investigate the combined influence of bottom currents and submarine landslides on seafloor morphology and sedimentary processes (Fig. 3). The specific objectives of this work are: (1) analyze the seafloor morphology and internal seismic characteristics of the moat-drift contourite system; (2) investigate its development processes and relationship with the Baiyun Slide scar; and (3) propose a conceptual model explaining the spatial and temporal interaction between bottom currents and submarine landslides.

GEOLOGIC AND OCEANOGRAPHIC SETTINGS

Geological setting

The South China Sea (SCS) is one of the largest and deepest marginal seas in the Western Pacific Ocean (Fig. 1). Located in the central part of the northern SCS, the Pearl River Mouth Basin (PRMB) spans an area of 17.5×10^4 km^2 , being repeated failed during the Baiyun Slide Complex since Quaternary (Yin *et al.*, 2019; Zhu *et al.*, 2019). During the Late Oligocene, continental breakup led to the formation of an extensive continental slope in the northern SCS, extending over 1000 km and accommodating substantial clastic deposits (Lin *et al.*, 2018). This period marked a transformative phase for the study area, transitioning from a shallow shelf environment (no more than 200 m deep) to a steep slope exceeding 3000 m in depth (Wang *et al.*, 2018).

The Pearl River delta front undergo successive developmental stages until Late Miocene, contributing to the formation of an unstable upper continental slope. (Lüdmann *et al.*, 2001; Jiang *et al.*, 2017; Wang *et al.*, 2018). At the same time, bottom currents intensified upper-slope instability by eroding the base of the slope, contributing to the collapse of the Pearl River distal prodelta region

(Zhu *et al.*, 2010; Zhou *et al.*, 2015; Jiang *et al.*, 2017). At the end of the Miocene, the Dongsha Tectonic Event was accompanied with localized uplift and faulting (Lüdmann & Wong, 1999; Lu *et al.*, 2017), reshaping the PRMB to the largest deep-water depocenter in the northern SCS (Wang *et al.*, 2018).

Oceanographic setting

Due to its semi-enclosed nature, the water column structure of SCS exhibits a complex pattern, including surface, intermediate, and deep water currents at least (Li *et al.*, 2013). Surface water currents, extending up to 500 m in depth, are primarily influenced by the East Asian monsoon, which drives a clockwise flow during summer and a counterclockwise movement in winter (Zhu *et al.*, 2010) (Fig. 2). Driven by the outflow of water to North Pacific, the clockwise intermediate water currents were established during the Late Miocene, occupying depths of 500 to 1500 m (Fig. 2). Deep-water currents, originating from the North Pacific, circulate counterclockwise at a depth exceeding 1500 m (Chen, 2005; Tian *et al.*, 2006; Yang *et al.*, 2010; Gong *et al.*, 2012).

DATA AND METHODS

The dataset used in this work comprises multibeam bathymetric and high-resolution 3D seismic data (Fig. 3). The 3D seismic data were acquired by the China National Offshore Oil Corporation (CNOOC) with a frequency of 40 Hz, a crossline spacing of 12.5 m, and a vertical sampling interval of 2 ms. These processes provide a vertical resolution of approximately 10-15 m at the depth relevant to this work. The high-resolution dataset enabled a detailed investigation of the sedimentary characteristics within the headwall area of the Baiyun Slide Complex.

Time-depth conversions were performed using average interval velocities of 1550 m/s for the water column and 1700 m/s for the shallow strata deposited since the Quaternary (Wang *et al.*, 2018). Multibeam bathymetric data were collected in water depths from 230 m to 2600 m and processed using CARIS HIPS® software. This processing resulted in a vertical resolution of 1-3.3 m and a horizontal resolution of approximately 100 m for the bathymetric data.

Schematic illustrations were used to facilitate a detailed interpretation and quantitative analysis of seafloor features in the study area (Fig. 4). Key morphological parameters were measured based on Miramontes et al. (2021) and Wilckens et al. (2023), including: (a) trough width, representing the horizontal distance from the drift crest to the slide scarp; (b) trough depth, which is the vertical distance from the base of the trough to the drift crest; and (c) drift crest, denoting the highest point of a mounded sedimentary body within the trough. Additionally, we define the scarp angle as the average gradient of the slide scarp, while the sediment angle represents the average gradient of the flank of the drift facing the slide scarp. These parameters provide measurements for the trough's width, depth, the position of the highest mounded sedimentary body, and the average angles between the base of the trough and the landslide scarp, or between the base of the trough and the drift crest, enabling precise quantification of the morphology of the main trough identified in the study area.

RESULTS

General seafloor morphology

The study area is located on the upper continental slope, directly below the shelf edge of the Pearl River Mouth Basin (Fig. 3). This region serve as a transitional zone between the broad, flat continental shelf and the continental slope. The shelf exhibits gradients typically less than 1° at depths of approximately 300 m (Fig. 3), while the western part of the slope exhibits a slightly steeper average inclination of around 2°. The headwall of the Baiyun Slide Complex is developed along this upper slope segment (Figs. 3 and 5). Approximately 15 km to the northeast, a large-scale system of submarine canyons, known as the Shenhu Canyon System, is observed (Fig. 3). These canyons trend perpendicularly to the shelf edge, extending downslope from the shallow shelf break to the base of the continental slope at a water depth of up to 2000 m.

Baiyun Slide scar

Multibeam bathymetric and 3D seismic data reveal that the geomorphology of the study area is markedly irregular, with the headwall scarp of the Baiyun Slide Complex being its most prominent feature (Figs. 5 and 6). This headwall scarp marks the location where upper slope failure occurs and downslope movement initiates. In the study area, this scarp extends approximately 45 km with a SSW-NNE orientation (Figs. 3 and 5). The headwall region of the Baiyun Slide Complex spans a water depth from 1100 m to 1600 m, being ~18 km long and 20 km wide, on average (Figs. 3 and 5). Morphologically, it has asymmetric concave and arcuate shapes, opening towards the east (Figs. 3 and 5). The average height of the slide scar's escarpment is approximately 90 m, with a maximum reaching 120 m (Fig. 5).

Slope gradient reveals uniformly low gradients (approximately 1°) both upslope and downslope of the escarpments of Baiyun Slide Complex. However, significant changes in slope angle are observed in the headwall region of the landslide at a water depth of 1100 m (Figs. 5 and 6), corresponding to the main failure initiation zone. Both transverse and longitudinal profiles record the highest gradients, approximately 15° (Figs. 6a and 6b), at the headwall scarp of the Baiyun Slide Complex (Fig. 6).

Downslope-oriented channel

Based on the analysis of multibeam and seismic data, several small-scale downslope-oriented channels (labeled C1 to C6) were identified on the upper continental slope above the headwall region of the Baiyun Slide Complex (Fig. 7a). These submarine channels are oriented perpendicularly to the main trend of the headwall scarp and generally follow a NE–SW course. Morphologically, these six (6) channels typically possess steep flanks and exhibit sinuous, groove-like features. Their length ranges from 6 to 38 km, their width from 800 to 1500 m, and incision depth varies from 20 to 60 m (Fig. 7b).

Seismic reflections across the six downslope-oriented channels are discontinuous, and erosional truncations are observed in strata along both channel flanks (Fig. 7c). Moreover, channels C1 and C2 incise the headwall escarpment of the Baiyun Slide Complex to extend eastward into the interior of the landslide domain. In particular, channel C2 follows a well-defined downslope path, incising deeply into the slide body. It is more than 15 km long and its incision depth reaches up to 60 m (Fig. 7a).

Along-slope-oriented trough

Analysis of bathymetric and seismic data reveals a prominent alongslope trough at the base of the headwall scarp of Baiyun Slide Complex (Figs. 8, 9 and 10). This trough, spanning water depths from 1100 m to 1350 m (Figs. 5 and 8a), is up to 600 m wide and 50 m deep (Figs. 8b, 8c, and 8d). It incises the headwall scarp of the Baiyun Slide Complex forming a distinct U-shaped notch at its base (Figs. 8b, 8c, and 8d). The trough aligns parallel to the headwall scarp (Fig. 8a) and shows discontinuous seismic reflections and erosional truncations on both its flanks (Figs. 9, 10a and 10b).

Quantitative measurements indicate that the angles of the headwall and sidewall scarps are significantly greater than those of the sediment accumulation surfaces within the trough (Figs. 8b, 8c, and 8d). Importantly, the trough developed exclusively in post-MTD sediments, overlying the top surface of the MTDs (Figs. 9a and 10a).

Sedimentary body within the scar

A sedimentary body with a thickness of up to 60 ms (two-way travel time, TWTT) is observed within the Baiyun Slide scar (Figs. 9a, 10a and 10b). It reveals a layered architecture and medium- to high-amplitude, sub-parallel internal seismic reflections demonstrating good lateral continuity. The proximal part of the sedimentary body is adjacent to the moat and shows localized mounded geometries, while the distal portion appears more tabular and laterally extensive. At the headwall scarp, seismic reflections from the sedimentary body terminate abruptly within the moat (Figs. 9 and 10). All in all, the sedimentary body becomes relatively flat farther away from the trough, exhibiting only minor undulations and slope angles of less than 1° (Figs. 9a and 10a).

Internal seismic reflection configuration

Seismic data illustrate that the slope is widely populated with a number of MTDs, some of which are concealed beneath thick sediment (Figs. 9b and 10a). These MTDs are characterized by discontinuous, chaotic, and transparent seismic facies, often with convoluted internal seismic reflections, particularly within the slide complex (Figs. 9b and 10a).

Sediments within the slide scar were transported from upper slope to lower slope, resulting in an expanding stack of MTDs when moving from west to east, thereby increasing the volume of the mass-wasted strata. Despite the overall downslope direction of movement, MTD thickness is greatest to the east. Compared to MTDs accumulated on the lower continental slope, discrete MTDs observed near the headwall are relatively thin (Fig. 9a).

DISCUSSION

Moat-drift contourite system near the Baiyun Slide scar

Seismic profiles across the study area reveal the presence of MTDs characterized by chaotic, transparent internal seismic reflections (Figs. 9 and 10a). Our findings indicate that the Baiyun Slide was only partially evacuated, resulting in the deposition of MTDs within the slide scar (Figs. 9 and 10). The Baiyun Slide Complex is estimated to have evacuated volume of approximately 1035 km^3 of sediment in four major MTDs (Sun et al., 2018). During the Quaternary, two major instability events occurred in the headwall area of the Baiyun Slide Complex (Li *et al.*, 2014; Wang *et al.*, 2017), dated to approximately 0.79 Ma and 0.54 Ma (Sun *et al.*, 2018). Notably, a 600 m wide and 50 m deep trough can still be identified along the escarpment of the Baiyun Slide Complex (Figs. 8b, 8c, and 8d).

Historically, geological literature has employed multiple terms to describe elongated troughs formed by marine geological processes. Faugères et al. (1999) used 'moat channels', while Hernández-Molina et al. (2006) described moats as elongated troughs primarily characterized by erosion and non-deposition. In our study area, key observations within the Baiyun Slide further delineate the observed trough: (1) it is oriented parallel to the slide margin and bounded by steep scarps on one side (Figs. 5 and 8); (2) seismic profiles exhibit erosional truncations adjacent to the headwall scarp of the Baiyun Slide Complex (Figs. 9 and 10); and (3) its main axis aligns with the flow direction of bottom currents (Figs. 3 and 8a). Such characteristics are highly consistent with the estabilished diagnostic criteria for moats (Hernández-Molina *et al.*, 2006; García *et al.*, 2009; Sayago-Gil *et al.*, 2010; Gong *et al.*, 2013; Miramontes *et al.*, 2021; Chen *et al.*, 2022). Therefore, we interpret the trough along the headwall scarp of the Baiyun Slide as a moat generated by erosion from alongslope bottom currents. This interpretation is supported by analogous features observed around seamounts in the Alboran Sea (Palomino *et al.*, 2011) and near the Maldives' carbonate platforms (Betzler *et al.*, 2013).

A distinct sedimentary body has been identified within the Baiyun Slide scar, stacked on top of the MTDs and comprising post-slide depositional features (Figs. 9 and 10). The term 'Sediment drift' refers to a depositional body formed by the accumulation of sediments influenced by alongslope bottom currents in deep-water environments (Stow *et al.*, 2002; Verdicchio & Trincardi, 2008). Based on their morphology and formative processes, sediment drifts are generally categorized into several types, including elongated, mounded drifts (Mulder *et al.*, 2006), sheeted drifts (Gao, 2020), and infilling drifts (Bryn *et al.*, 2005). In the study area, sediment drifts developed within the Baiyun Slide scar exhibit excellent lateral continuity (Figs. 9 and 10). They are recognized by distinct sediment mounds near the distal end of the moat, where seismic reflections bend downslope toward the moat's deepest part (Figs. 9 and 10). This seismic character aligns with established diagnostic criteria for infilling drifts (Faugères *et al.*, 1999; Stow *et al.*, 2002; Rebesco & Camerlenghi, 2008; Miramontes *et al.*, 2021; Wilckens *et al.*, 2023). Accordingly, the observed sedimentary body is classified as an infilling drift (Faugères *et al.*, 1999; Bryn *et al.*, 2005; Rebesco & Camerlenghi, 2008).

Moats and sediment drifts are often intricately linked, leading scholars to consider them as a joint entity known as a moat-drift contourite system (e.g., Wilckens *et al.*, 2023; Zhao *et al.*, 2024). Building on this fact, we propose that a moat-drift contourite system developed within the Baiyun Slide scar after the emplacement of the Baiyun Slide Complex. This system indicates that post-slide sedimentation in this area was significantly influenced by alongslope bottom currents. Therefore, we conclude that the Baiyun Slide and alongslope bottom currents jointly sculpted the seafloor morphology in this region.

The role of slide scarps in the initiation of moat-drift contourite systems

Seismic data reveal the absence of any pre-existing moat-drift contourite systems underneath the basal shear zone of the observed MTDs in the study area (Figs. 9 and 10a). Crucially, both the moat and the sediment drift develop exclusively just above the MTDs' top surface (Figs. 9a and 10a), confirming that the moat and sediment drift within the Baiyun Slide scar post-date the emplacement of the Baiyun Slide. Therefore, we propose that the studied moat-drift contourite system is closely associated with alongslope bottom currents and was initiated by the presence of the Baiyun Slide scar.

Our study area spans water depths from 800 to 1500 m, placing it within the influence of intermediate water masses (Fig. 2). Previous studies have demonstrated the crucial role of seafloor topography in influencing local water mass distribution and the flow paths of alongslope bottom currents (Palomino *et al.*, 2011; Ercilla *et al.*, 2016; Rebesco *et al.*, 2016). Thus, we propose that the Baiyun Slide Complex remobilized substantial volumes of sediment, thereby forming a permanent negative bathymetric feature that resulted in the formation of pronounced sidewall and headwall scarps. We infer that this significantly altered the flow paths and depositional patterns of bottom currents in the study area. As intermediate water flows from southwest to northeast along the continental slope in a permanent clockwise direction (Zhu *et al.*, 2010; Li *et al.*, 2013), it generated a branch that flows across the headwall of the Baiyun Slide, following the slope morphology, and subsequently flowing out the Baiyun Slide scar. Similar hydrodynamic behavior has been documented in the Kveithola Trough in the Northwest Barents Sea (Rebesco *et al.*, 2016) and along the Spanish Slope (Ercilla *et al.*, 2016). In these settings, bottom currents are inferred to enter slope depressions, follow contour-parallel paths within the confined topography, and subsequently exit along the deepest part of the trough.

Bottom current velocity along the continental slope is strongly affected by seafloor morphology (Ercilla *et al.*, 2016; García *et al.*, 2016; Thiéblemont *et al.*, 2019). A number of studies have confirmed that slide scars are preferential areas for enhanced bottom current activity (Bryn *et al.*, 2005; Laberg *et al.*, 2005; Masson *et al.*, 2006; Van Rooij *et al.*, 2010; García *et al.*, 2016; Martorelli *et al.*, 2016). When encountering steep scarps, seamounts, or other morphological obstacles, the velocity of bottom currents can increase by a factor of two or more (Sun *et al.*, 2016; Zhang *et al.*, 2016). Documented cases include an acceleration of bottom currents from 10 cm/s to 25 cm/s due to the presence of Le Danois Bank and Vizco High (Liu *et al.*, 2019), a similar increase in bottom current velocities in northwest Iberia from 7 cm/s to 35 cm/s (Zhang *et al.*, 2016), and in the Xisha Trough from 15 cm/s to 30 cm/s (Chen *et al.*, 2016). We propose that the steep headwall scarps of the Baiyun Slide have acted as morphological barriers that increased bottom-current velocity. This intensified bottom current activity eroded unconsolidated sediment on the seafloor, or prevented its depositon, leading to the formation of erosional or non-depositional features such as the moat (Rebesco & Camerlenghi, 2008; Liu *et al.*, 2019; Thiéblemont *et al.*, 2019). Examples from the northern Campos slope on the southwestern Atlantic margin (Viana *et al.*, 2002) and the shelf edge of Alboran Sea in the southwestern Mediterranean (Ercilla *et al.*, 2016) further support this interpretation.

Sediment drifts represent important alongslope accumulations of sediment (Ercilla *et al.*, 2016; Thiéblemont *et al.*, 2019). In the study area, sediment drifts filled the Baiyun Slide scar, but demonstrating clear spatial differences: erosional features are observed near the moat, while depositional features become increasingly important farther away from the moat (Figs. 9a and 10). Such distinct erosional and sedimentary features serve as good indicators of water-mass intensity (Mccave & Carter, 1997; Palomino *et al.*, 2011). Hence, we propose that in areas without obstacles such as scarps, bottom-current velocity may not be significantly enhanced, allowing deposition to primarily occur in regions with relatively low current velocities. Over time, suspended sediment particles settle out of the water column, leading to the formation of a sediment drift (Rebesco *et al.*, 2014; Cattaneo *et al.*, 2017). Eventually, sediment was accumulated on the seafloor and filled the accommodation space generated by the Baiyun Slide Complex. Furthermore, the seismic reflections close to the moat show mounded shapes (Figs. 7b and 8a), which are most likely attributed to the presence of the headwall scarp. This suggests that enhanced bottom currents not only intensified seafloor erosion or non-deposition but also led to the significant resuspension and redistribution of sediments (Cacchione *et al.*, 2002; Pomar *et al.*, 2012; Thiéblemont *et al.*, 2019). Sediment was deposited on one side of the moat, causing the drift to stack vertically, which explains the remarkable mounded shapes observed in the sediment drift near the moat.

The modern oceanographic framework of the South China Sea has remained stable for approximately 3 Ma, with the northern continental margin consistently influenced by the intermediate water mass for an extended period (Zhu *et al.*, 2010; Liu *et al.*, 2011; Li *et al.*, 2013; Sun *et al.*, 2016). Alongslope bottom currents associated with ocean circulation flow extensively within a given depth range and remain stable over geological time, with their presence clearly identifiable in the sedimentary record (Rebesco *et al.*, 2014; Miramontes *et al.*, 2021; Rodrigues *et al.*, 2022). Therefore, we propose that the persistent alongslope bottom currents in the northern South China Sea interacted with the Baiyun Slide scar, leading to alternating contourite deposition and erosion, and profoundly altering the seafloor morphology in the study area.

IMPLICATIONS

A conceptual model for slide-controlled moat–drift contourite systems

Based on a detailed interpretation of multibeam bathymetric and seismic data, we develop a conceptual model to explain the evolution of seafloor morphology in our study area (Fig. 11). The initial emplacement of the Baiyun Slide resulted in the formation of negative topography and steep escarpments. We infer that this was followed by the branching and along-contour flow of intermediate water mass along the contours within the headwall region (Fig. 11a). Subsequently, localized acceleration of bottom-current velocity along the slide escarpment led to sediment erosion and/or non-deposition, initiating and driving the development of the moat (Fig. 11b). In contrast, regions located away from these escarpments experienced decreased bottom flow velocity, resulting in the generation of infilling drifts (Fig. 11c).

In the field of marine geology, contourites refer to sediments deposited or significantly reworked under the persistent influence of bottom currents (Rebesco & Camerlenghi, 2008; Rebesco *et al.*, 2014). A moat–drift contourite system represents a composite depositional system that includes both erosional (e.g., moats, furrows) and depositional (e.g., drifts) features associated with contourite processes (Hernández-Molina *et al.*, 2006; Rebesco *et al.*, 2014). In our study area, the moat develops along the headwall escarpment of the Baiyun Slide Complex, while the infilling drift accumulated within the slide scar, jointly constituting the full expression of a moat–drift contourite system. In this context, bottom currents serve as the principal driving mechanism for the initiation and evolution of the system. The steep escarpment generated by the Baiyun Slide acts as a prominent bathymetric obstacle, altering the flow pathway and intensifying current velocity along the slope break. This hydrodynamic focusing promotes erosion and leads to the incision of the moat. In contrast, in areas farther from the escarpment, where current velocity remains lower, the negative topography created by the submarine landslide traps suspended sediments, facilitating their accumulation as infilling drifts.

Previous studies have documented the presence of moat-drift contourite systems in various geological settings, including open continental slopes (Alves, 2010; Vandorpe *et al.*, 2014;

Miramontes *et al.*, 2016; Liu *et al.*, 2020), around seamounts (Howe *et al.*, 2006; Palomino *et al.*, 2011; Chen *et al.*, 2014) and carbonate mounds (Micallef *et al.*, 2009; Betzler *et al.*, 2013). However, this study confirms that submarine landslides represent a key mechanism in the formation of moat–drift contourite systems in deep-water environments. We therefore propose the term "Slide-controlled Moat–drift Contourite System" for this type of depositional system. The conceptual model presented here may also explain the initiation and evolution of similar slide-related moat-drift contourite systems globally (Bryn *et al.*, 2005; Laberg *et al.*, 2005; Masson *et al.*, 2006; Van Rooij *et al.*, 2010). Given the widespread occurrence of submarine landslides across continental margins affected by bottom currents, on both passive and active margins (Rebesco *et al.*, 2014; Li *et al.*, 2020), we propose that moat-drift contourite systems influenced by submarine landslides might be more frequent and extensive in the geological record than previously recognized. Such systems could occur not only in currently active seafloor settings but also in buried and exhumed stratigraphic successions.

Slide-controlled secondary contourite systems

We propose that the broader slope region surrounding the Baiyun Slide Complex represents a sedimentary environment predominantly governed by gravity-driven downslope sedimentary processes. Multiple independent datasets support this interpretation: (1) Detailed analysis of multibeam bathymetric and 3D seismic profiles reveal a series of small-scale submarine channels (C1–C6) incised into the upper slope near the continental shelf break above the Baiyun Slide Complex (Figs. 5, 7, 9b ,10a). Channels C1 and C2 cut through the headwall scarp and extend downslope into the interior of the slide scar, with lengths of up to 15 km and incision depths reaching 60 m (Figs. 8b and 9b), indicating sustained influence from sediment gravity flows. (2) Wang et al. (2018) analyzed piston cores (P1, P2, P3, P4) collected from the upper slope above the headwall of the Baiyun Slide and identified abundant turbidite deposits, suggesting frequent deposition by downslope gravity flows. (3) The Baiyun Slide itself represents a large-scale mass-transport event, one of the most prominent gravity-flow features along the northern South China Sea margin, and has played a key role in sediment reworking and redistribution across the region. (4) Approximately 15 km northeast of the Baiyun Slide Complex, the Shenhu Canyon System exhibits a deeply incised, multi-branch morphology, reflecting long-term and voluminous downslope gravity-flow activity (Yu *et al.*, 2014).

However, our observations reveal the development of a local sedimentary system dominated by bottom-current activity. This secondary depositional system, confined within the topographic depression generated by the Baiyun Slide, contrasts markedly with the regional downslope sedimentary regime and reflects a spatial shift in the dominant sedimentary process from downslope to alongslope control. The presence of infilling drifts and a well-defined moat formed along the slide scar escarpment provides compelling evidence that bottom currents, rather than gravity flows, have played the primary role in sediment transport and deposition within this specific geomorphological context. The formation of the steep escarpment reoriented bottom current pathways thereby enhancing sediment reworking and promoting the development of depositional features that are decoupled from the downslope gravity-flow processes. We interpret this as a localized reorganization of sedimentary processes, induced by the topographic transformation caused by the landslide event. To describe this phenomenon, we introduce the concept of a slide-controlled secondary contourite depositional system. This system develops within a larger gravity-flow-dominated continental slope, yet it exhibits clear sedimentological and morphological signatures typical of contourite processes, such as moat, associated infilling drift, and erosional truncation surfaces. The proposed conceptual model highlights a cascade of interactions.

Based on our findings, this distinction between primary (gravity flow-dominated) and secondary (bottom current-controlled) depositional systems within a single slope domain offers a novel perspective on sediment partitioning in tectonically and morphodynamically active continental margins. Our results further underscore the role of submarine landslides not only as sediment delivery mechanisms, but also as morphodynamic agents capable of reconfiguring deep-marine flow fields and fostering the development of bottom current driven systems within otherwise gravity-dominated environments.

CONCLUSIONS

This study utilizes multibeam bathymetric and 3D seismic data to investigate the geomorphological features associated with the Bayiun Slide Complex on the northern South China Sea margin. Our primary objective is to understand the initiation and evolution of a potentially understudied moat-drift contourite system linked to submarine landslides, by identifying the main sedimentary processes and analyzing the comprehensive impact of submarine landslides on alongslope bottom currents. The key findings and conclusions of this study are as follows:

(1) A disntinct slide-controlled moat–drift contourite system has been identified within the Baiyun Slide scar. This system comprises a 600 m-wide, 50 m-deep moat adjacent to the steep slide escarpment and a ~54 m-thick sediment drift deposited in the interior of the scar.

(2) Near the slide escarpment, the velocity of alongslope bottom currents intensifies, promoting turbulence and erosion, which facilitated the initiation and development of the moat. In contrast, in areas more distal to the slide scarp, bottom currents are less intense, allowing for the settling of resuspended particles and the formation of the sediment drift.

(3) Although the broader slope region surrounding the Baiyun Slide Complex is predominantly governed by gravity-driven sedimentary processes, the development of this moat–drift contourite system within the slide scar reveals a localized, slide-controlled secondary sedimentary system dominated by bottom-current activity. This finding underscores the capacity of submarine landslides to reconfigure local sedimentary regimes, facilitating a transition from downslope to alongslope depositional processes in deep-marine environments.

(4) Based on these observations, we propose a new conceptual model for slide-controlled secondary contourite systems, offering a mechanistic explanation for similar features observed globally. This model not only explains the genesis of such systems but also emphasizes the morphodynamic role of submarine landslides in enabling bottom-current-driven sedimentation in otherwise gravity-dominated environments.

(5) The sedimentary architecture of such hybrid systems provides valuable archives for reconstructing past changes in ocean circulation and slope instability. Given the widespread occurrence of submarine landslides and bottom currents across passive and active margins, slide-controlled contourite systems may be more common in the geological records than previously recognized.

ACKNOWLEDGEMENTS

The authors acknowledge CNOOC for providing access to the geophysical data used in this research. This research was financially supported by National Engineering Research Center of Gas Hydrate Exploration and Development (No. NERCZ202402), National Natural Science Foundation of China (U22B20126), the National Key Research and Development Program (2022YFC2806100), National Natural Science Foundation of China (No. 42306070), and the Guangzhou Basic and Applied Basic Research Program (No. 2024A04J3812). We thank the Chief Editor Dr. Piret Plink-Björklund, Associate Editor Dr. Victoria Valdez Buso, Dr. Kei Ogata, Dr. Francisco Javier Hernández-Molina and one anonymous reviewer for their positive comments which helped us improve our manuscript.

REFERENCES

Alves, T.M. (2010) A 3-D morphometric analysis of erosional features in a contourite drift from offshore SE Brazil: Morphometric analysis of erosional features. *Geophysical Journal International*, **183**, 1151–1164.

Armitage, D.A., **Romans, B.W.**, **Covault, J.A.** and **Graham, S.A.** (2009) The Influence of Mass-Transport-Deposit Surface Topography on the Evolution of Turbidite Architecture: The Sierra Contreras, Tres Pasos Formation (Cretaceous), Southern Chile. *Journal of Sedimentary Research*, **79**, 287–301.

Betzler, C., **Lüdmann, T.**, **Hübscher, C.** and **Fürstenau, J.** (2013) Current and sea-level signals in periplatform ooze (Neogene, Maldives, Indian Ocean). *Sedimentary Geology*, **290**, 126–137.

Bryn, P., **Berg, K.**, **Stoker, M.S.**, **Haflidason, H.** and **Solheim, A.** (2005) Contourites and their relevance for mass wasting along the Mid-Norwegian Margin. *Marine and Petroleum Geology*, **22**, 85–96.

Cacchione, D.A., **Pratson, L.F.** and **Ogston, A.S.** (2002) The Shaping of Continental Slopes by Internal Tides. *Science*, **296**, 724–727.

Cattaneo, A., **Miramontes, E.**, **Samalens, K.**, **Garreau, P.**, **Caillaud, M.**, **Marsset, B.**, **Corradi, N.** and **Migeon, S.** (2017) Contourite identification along Italian margins: The case of the Portofino drift (Ligurian Sea). *Marine and Petroleum Geology*, **87**, 137–147.

Chen, C.-T.A. (2005) Tracing tropical and intermediate waters from the South China Sea to the Okinawa Trough and beyond. *J. Geophys. Res.*, **110**, C05012.

Chen, H., **Xie, X.**, **Van Rooij, D.**, **Vandorpe, T.**, **Su, M.** and **Wang, D.** (2014) Depositional characteristics and processes of alongslope currents related to a seamount on the northwestern margin of the Northwest Sub-Basin, South China Sea. *Marine Geology*, **355**, 36–53.

Chen, H., **Xie, X.**, **Zhang, W.**, **Shu, Y.**, **Wang, D.**, **Vandorpe, T.** and **Van Rooij, D.** (2016) Deep-water sedimentary systems and their relationship with bottom currents at the intersection of Xisha Trough and Northwest Sub-Basin, South China Sea. *Marine Geology*, **378**, 101–113.

Chen, H., **Zhang, W.**, **Xie, X.**, **Gao, Y.**, **Liu, S.**, **Ren, J.**, **Wang, D.** and **Su, M.** (2022) Linking oceanographic processes to contourite features: Numerical modelling of currents influencing a contourite depositional system on the northern South China Sea margin. *Marine Geology*, **444**, 106714.

Ercilla, G., **Juan, C.**, **Hernández-Molina, F.J.**, **Bruno, M.**, **Estrada, F.**, **Alonso, B.**, **Casas, D.**, **Farran, Marcel. lí**, **Llave, E.**, **García, M.**, **Vázquez, J.T.**, **D'Acremont, E.**, **Gorini, C.**, **Palomino, D.**, **Valencia, J.**, **El Moumni, B.** and **Ammar, A.** (2016) Significance of bottom currents in deep-sea morphodynamics: An example from the Alboran Sea. *Marine Geology*, **378**, 157–170.

Faugères, J.-C., **Stow, D.A.V.**, **Imbert, P.** and **Viana, A.** (1999) Seismic features diagnostic of contourite drifts. *Marine Geology*, **162**, 1–38.

Gao, Y. (2020) Seismic stratigraphy and deep-water sedimentary evolution of the southern Mozambique margin_ Central Terrace and Mozambique Fracture Zone. *Marine Geology*, 18.

García, M., **Hernández-Molina, F.J.**, **Alonso, B.**, **Vázquez, J.T.**, **Ercilla, G.**, **Llave, E.** and **Casas, D.** (2016) Erosive sub-circular depressions on the Guadalquivir Bank (Gulf of Cadiz): Interaction between bottom current, mass-wasting and tectonic processes. *Marine Geology*, **378**, 5–19.

García, M., **Hernández-Molina, F.J.**, **Llave, E.**, **Stow, D.A.V.**, **León, R.**, **Fernández-Puga, M.C.**, **Diaz Del Río, V.** and **Somoza, L.** (2009) Contourite erosive features caused by the Mediterranean Outflow Water in the Gulf of Cadiz: Quaternary tectonic and oceanographic implications. *Marine Geology*, **257**, 24–40.

Gatter, R., **Clare, M.A.**, **Kuhlmann, J.** and **Huhn, K.** (2021) Characterisation of weak layers, physical controls on their global distribution and their role in submarine landslide formation. *Earth-Science Reviews*, **223**, 103845.

Gong, C., **Wang, Y.**, **Peng, X.**, **Li, W.**, **Qiu, Y.** and **Xu, S.** (2012) Sediment waves on the South China Sea Slope off southwestern Taiwan: Implications for the intrusion of the Northern Pacific Deep Water into the South China Sea. *Marine and Petroleum Geology*, **32**, 95–109.

Gong, C., **Wang, Y.**, **Zhu, W.**, **Li, W.** and **Xu, Q.** (2013) Upper Miocene to Quaternary unidirectionally migrating deep-water channels in the Pearl River Mouth Basin, northern South China Sea. *Bulletin*, **97**, 285–308.

Heerema, C.J., **Talling, P.J.**, **Cartigny, M.J.**, **Paull, C.K.**, **Bailey, L.**, **Simmons, S.M.**, **Parsons, D.R.**, **Clare, M.A.**, **Gwiazda, R.**, **Lundsten, E.**, **Anderson, K.**, **Maier, K.L.**, **Xu, J.P.**, **Sumner, E.J.**, **Rosenberger, K.**, **Gales, J.**, **McGann, M.**, **Carter, L.** and **Pope, E.** (2020) What determines the downstream evolution of turbidity currents? *Earth and Planetary Science Letters*, **532**, 116023.

Hernández-Molina, F.J., **Llave, E.**, **Stow, D.A.V.**, **García, M.**, **Somoza, L.**, **Vázquez, J.T.**, **Lobo, F.J.**, **Maestro, A.**, **Díaz Del Río, V.**, **León, R.**, **Medialdea, T.** and **Gardner, J.** (2006) The contourite depositional system of the Gulf of Cádiz: A sedimentary model related to the bottom current activity of the Mediterranean outflow water and its interaction with the continental margin. *Deep Sea Research Part II: Topical Studies in Oceanography*, **53**, 1420–1463.

Hernández-Molina, F.J., **Serra, N.**, **Stow, D.A.V.**, **Llave, E.**, **Ercilla, G.** and **Van Rooij, D.** (2011) Along-slope oceanographic processes and sedimentary products around the Iberian margin. *Geo-Mar Lett*, **31**, 315–341.

Hernández-Molina, J., **Llave, E.**, **Somoza, L.**, **Fernández-Puga, M.C.**, **Maestro, A.**, **León, R.**, **Medialdea, T.**, **Barnolas, A.**, **García, M.**, **Del Río, V.D.**, **Fernández-Salas, L.M.**, **Vázquez, J.T.**, **Lobo, F.**, **Dias, J.M.A.**, **Rodero, J.** and **Gardner, J.** (2003) Looking for clues to paleoceanographic imprints: A diagnosis of the Gulf of Cadiz contourite depositional systems. *Geol*, **31**, 19.

Howe, J.A., **Stoker, M.S.**, **Masson, D.G.**, **Pudsey, C.J.**, **Morris, P.**, **Larter, R.D.** and **Bulat, J.** (2006) Seabed morphology and the bottom-current pathways around Rosemary Bank seamount, northern Rockall Trough, North Atlantic. *Marine and Petroleum Geology*, **23**, 165–181.

Hutton, E.W.H. and **Syvitski, J.P.M.** (2004) Advances in the numerical modeling of sediment failure during the development of a continental margin. *Marine Geology*, **203**, 367–380.

Jiang, J., **Shi, H.**, **Lin, C.**, **Zhang, Z.**, **Wei, A.**, **Zhang, B.**, **Shu, L.**, **Tian, H.**, **Tao, Z.** and **Liu, H.** (2017) Sequence architecture and depositional evolution of the Late Miocene to quaternary northeastern shelf margin of the South China Sea. *Marine and Petroleum Geology*, **81**, 79–97.

Juan, C., **Van Rooij, D.** and **De Bruycker, W.** (2018) An assessment of bottom current controlled sedimentation in Pacific Ocean abyssal environments. *Marine Geology*, **403**, 20–33.

Kneller, B., **Dykstra, M.**, **Fairweather, L.** and **Milana, J.P.** (2016) Mass-transport and slope accommodation: Implications for turbidite sandstone reservoirs. *Bulletin*, **100**, 213–235.

Kremer, C.H., **McHargue, T.**, **Scheucher, L.** and **Graham, S.A.** (2018) Transversely-sourced mass-transport deposits and stratigraphic evolution of a foreland submarine channel system: Deep-water tertiary strata of the Austrian Molasse Basin. *Marine and Petroleum Geology*, **92**, 1–19.

Laberg, J.S., **Stoker, M.S.**, **Dahlgren, K.I.T.**, **Haas, H. de**, **Haflidason, H.**, **Hjelstuen, B.O.**, **Nielsen, T.**, **Shannon, P.M.**, **Vorren, T.O.**, **van Weering, T.C.E.** and **Ceramicola, S.** (2005) Cenozoic alongslope processes and sedimentation on the NW European Atlantic margin. *Marine and Petroleum Geology*, **22**, 1069–1088.

Li, H., **Wang, Y.**, **Zhu, W.**, **Xu, Q.**, **He, Y.**, **Tang, W.**, **Zhuo, H.**, **Wang, D.**, **Wu, J.** and **Li, D.** (2013) Seismic characteristics and processes of the Plio-Quaternary unidirectionally migrating channels and contourites in the northern slope of the South China Sea. *Marine and Petroleum Geology*, **43**, 370–380.

Li, W., **Alves, T.M.**, **Rebesco, M.**, **Sun, J.**, **Li, J.**, **Li, S.** and **Wu, S.** (2020) The Baiyun Slide Complex, South China Sea: A modern example of slope instability controlling submarine-channel incision on continental slopes. *Marine and Petroleum Geology*, **114**, 104231.

Li, W., **Wu, S.**, **Völker, D.**, **Zhao, F.**, **Mi, L.** and **Kopf, A.** (2014) Morphology, seismic characterization and sediment dynamics of the Baiyun Slide Complex on the northern South China Sea margin. *JGS*, **171**, 865–877.

Lin, C., **Jiang, J.**, **Shi, H.**, **Zhang, Z.**, **Liu, J.**, **Qin, C.**, **Li, H.**, **Ran, H.**, **Wei, A.**, **Tian, H.**, **Xing, Z.** and **Yao, Q.** (2018) Sequence architecture and depositional evolution of the northern continental slope of the South China Sea: responses to tectonic processes and changes in sea level. *Basin Res*, **30**, 568–595.

Lintern, D.G., **Hill, P.R.** and **Stacey, C.** (2016) Powerful unconfined turbidity current captured by cabled observatory on the Fraser River delta slope, British Columbia, Canada. *Sedimentology*, **63**, 1041–1064.

Liu, G., **Wang, D.**, **Chen, W.**, **Wang, W.**, **Betzler, C.** and **Han, X.** (2023) Submarine landslides on a carbonate platform slope changing transport pathways of deepwater gravity flows: Insights from the Xisha Islands, South China Sea. *Geomorphology*, **437**, 108813.

Liu, J., **Xiang, R.**, **Chen, M.**, **Chen, Z.**, **Yan, W.** and **Liu, F.** (2011) Influence of the Kuroshio current intrusion on depositional environment in the Northern South China Sea: Evidence from surface sediment records. *Marine Geology*, **285**, 59–68.

Liu, S., **Hernández-Molina, F.J.**, **Ercilla, G.** and **Van Rooij, D.** (2020) Sedimentary evolution of the Le Danois contourite drift systems (southern Bay of Biscay, NE Atlantic): A reconstruction of the Atlantic Mediterranean Water circulation since the Pliocene. *Marine Geology*, **427**, 106217.

Liu, S., **Van Rooij, D.**, **Vandorpe, T.**, **González-Pola, C.**, **Ercilla, G.** and **Hernández-Molina, F.J.** (2019) Morphological features and associated bottom-current dynamics in the Le Danois Bank region (southern Bay of Biscay, NE Atlantic): A model in a topographically constrained small basin. *Deep Sea Research Part I: Oceanographic Research Papers*, **149**, 103054.

Lu, Y., **Luan, X.**, **Lyu, F.**, **Wang, B.**, **Yang, Z.**, **Yang, T.** and **Yao, G.** (2017) Seismic evidence and formation mechanism of gas hydrates in the Zhongjiannan Basin, Western margin of the South China Sea. *Marine and Petroleum Geology*, **84**, 274–288.

Lüdmann, T., **Kin Wong, H.** and **Wang, P.** (2001) Plio–Quaternary sedimentation processes and neotectonics of the northern continental margin of the South China Sea. *Marine Geology*, **172**, 331–358.

Lüdmann, T. and **Wong, H.K.** (1999) Neotectonic regime on the passive continental margin of the northern South China Sea. *Tectonophysics*, **311**, 113–138.

Martorelli, E., **Bosman, A.**, **Casalbore, D.** and **Falcini, F.** (2016) Interaction of down-slope and along-slope processes off Capo Vaticano (southern Tyrrhenian Sea, Italy), with particular reference to contourite-related landslides. *Marine Geology*, **378**, 43–55.

Masson, D.G., **Harbitz, C.B.**, **Wynn, R.B.**, **Pedersen, G.** and **Løvholt, F.** (2006) Submarine landslides: processes, triggers and hazard prediction. *Phil. Trans. R. Soc. A.*, **364**, 2009–2039.

McAdoo, B.G., **Pratson, L.F.** and **Orange, D.L.** (2000) Submarine landslide geomorphology, US continental slope. *Marine Geology*, **169**, 103–136.

Mccave, I.N. and **Carter, L.** (1997) Recent sedimentation beneath the Deep Western Boundary Current off northern New Zealand. *Deep Sea Research Part I: Oceanographic Research Papers*, **44**, 1203–1237.

Micallef, A., **Masson, D.G.**, **Berndt, C.** and **Stow, D.A.V.** (2009) Development and mass movement processes of the north-eastern Storegga Slide. *Quaternary Science Reviews*, **28**, 433–448.

Minisini, D., **Trincardi, F.** and **Asioli, A.** (2006) Evidence of slope instability in the Southwestern Adriatic Margin. *Nat. Hazards Earth Syst. Sci.*, **6**, 1–20.

Miramontes, E., **Cattaneo, A.**, **Jouet, G.**, **Théreau, E.**, **Thomas, Y.**, **Rovere, M.**, **Cauquil, E.** and **Trincardi, F.** (2016) The Pianosa Contourite Depositional System (Northern Tyrrhenian Sea): Drift morphology and Plio-Quaternary stratigraphic evolution. *Marine Geology*, **378**, 20–42.

Miramontes, E., **Garreau, P.**, **Caillaud, M.**, **Jouet, G.**, **Pellen, R.**, **Hernández-Molina, F.J.**, **Clare, M.A.** and **Cattaneo, A.** (2019) Contourite distribution and bottom currents in the NW Mediterranean Sea: Coupling seafloor geomorphology and hydrodynamic modelling. *Geomorphology*, **333**, 43–60.

Miramontes, E., **Thiéblemont, A.**, **Babonneau, N.**, **Penven, P.**, **Raisson, F.**, **Droz, L.**, **Jorry, S.J.**, **Fierens, R.**, **Counts, J.W.**, **Wilckens, H.**, **Cattaneo, A.** and **Jouet, G.** (2021) Contourite and mixed turbidite-contourite systems in the Mozambique Channel (SW Indian Ocean): Link between geometry, sediment characteristics and modelled bottom currents. *Marine Geology*, **437**, 106502.

Mosher, D.C. and **Boggild, K.** (2021) Impact of bottom currents on deep water sedimentary processes of Canada Basin, Arctic Ocean. *Earth and Planetary Science Letters*, **569**, 117067.

Mulder, T., **Gonthier, E.**, **Lecroart, P.**, **Hanquiez, V.**, **Marches, E.** and **Voisset, M.** (2009) Sediment failures and flows in the Gulf of Cadiz (eastern Atlantic). *Marine and Petroleum Geology*, 13.

Mulder, T., **Lecroart, P.**, **Hanquiez, V.**, **Marches, E.**, **Gonthier, E.**, **Guedes, J.-C.**, **Thiébot, E.**, **Jaaidi, B.**, **Kenyon, N.**, **Voisset, M.**, **Perez, C.**, **Sayago, M.**, **Fuchey, Y.** and **Bujan, S.** (2006) The western part of the Gulf of Cadiz: contour currents and turbidity currents interactions. *Geo-Mar Lett*, **26**, 31–41.

Normandeau, A., **Campbell, D.C.**, **Piper, D.J.W.** and **Jenner, K.A.** (2019) Are submarine landslides an underestimated hazard on the western North Atlantic passive margin? *Geology*, **47**, 848–852.

Ogata, K., **Mountjoy, J.J.**, **Pini, G.A.**, **Festa, A.** and **Tinterri, R.** (2014) Shear zone liquefaction in mass transport deposit emplacement: A multi-scale integration of seismic reflection and outcrop data. *Marine Geology*, **356**, 50–64.

Ogata, K., **Mutti, E.**, **Pini, G.A.** and **Tinterri, R.** (2012) Mass transport-related stratal disruption within sedimentary mélanges: Examples from the northern Apennines (Italy) and south-central Pyrenees (Spain). *Tectonophysics*, **568–569**, 185–199.

Palomino, D., **Vázquez, J.-T.**, **Ercilla, G.**, **Alonso, B.**, **López-González, N.** and **Díaz-del-Río, V.** (2011) Interaction between seabed morphology and water masses around the seamounts on the Motril Marginal Plateau (Alboran Sea, Western Mediterranean). *Geo-Mar Lett*, **31**, 465–479.

Pomar, L., **Morsilli, M.**, **Hallock, P.** and **Bádenas, B.** (2012) Internal waves, an under-explored source of turbulence events in the sedimentary record. *Earth-Science Reviews*, **111**, 56–81.

Qin, Y., **Alves, T.M.**, **Constantine, J.** and **Gamboa, D.** (2017) The Role of Mass Wasting In the Progressive Development Of Submarine Channels (Espírito Santo Basin, Se Brazil). *Journal of Sedimentary Research*, **87**, 500–516.

Rebesco, M. and **Camerlenghi, A.** (2008) Late Pliocene margin development and mega debris flow deposits on the Antarctic continental margins: Evidence of the onset of the modern Antarctic Ice Sheet? *Palaeogeography, Palaeoclimatology, Palaeoecology*, **260**, 149–167.

Rebesco, M., **Hernández-Molina, F.J.**, **Van Rooij, D.** and **Wåhlin, A.** (2014) Contourites and associated sediments controlled by deep-water circulation processes: State-of-the-art and future considerations. *Marine Geology*, **352**, 111–154.

Rebesco, M., **Özmaral, A.**, **Urgeles, R.**, **Accettella, D.**, **Lucchi, R.G.**, **Rüther, D.**, **Winsborrow, M.**, **Llopart, J.**, **Caburlotto, A.**, **Lantzsch, H.** and **Hanebuth, T.J.J.** (2016) Evolution of a high-latitude sediment drift inside a glacially-carved trough based on high-resolution seismic stratigraphy (Kveithola, NW Barents Sea). *Quaternary Science Reviews*, **147**, 178–193.

Rodrigues, S., **Hernández-Molina, F.J.**, **Fonnesu, M.**, **Miramontes, E.**, **Rebesco, M.** and **Campbell, D.C.** (2022) A new classification system for mixed (turbidite-contourite) depositional systems: Examples, conceptual models and diagnostic criteria for modern and ancient records. *Earth-Science Reviews*, **230**, 104030.

Sayago-Gil, M., **Long, D.**, **Hitchen, K.**, **Díaz-del-Río, V.**, **Fernández-Salas, L.M.** and **Durán-Muñoz, P.** (2010) Evidence for current-controlled morphology along the western slope of Hatton Bank (Rockall Plateau, NE Atlantic Ocean). *Geo-Mar Lett*, **30**, 99–111.

Shanmugam, G. (2021) Deep-Water Processes and Deposits. In: *Encyclopedia of Geology, Elsevier*, 965–1009.

Smoot, N.C. and **King, R.E.** (1993) Three-dimensional secondary surface geomorphology of submarine landslides on northwest Pacific plate guyots. *Geomorphology*, **6**, 151–173.

Stagna, M.D., **Maselli, V.** and **Van Vliet, A.** (2023) Large-scale submarine landslide drives long-lasting regime shift in slope sediment deposition. *Geology*, **51**, 167–173.

Stow, D.A.V., **Faugères, J.-C.**, **Howe, J.A.**, **Pudsey, C.J.** and **Viana, A.R.** (2002) Bottom currents, contourites and deep-sea sediment drifts: current state-of-the-art. *Memoirs*, **22**, 7–20.

Sun, Q., **Cartwright, J.**, **Wu, S.**, **Zhong, G.**, **Wang, S.** and **Zhang, H.** (2016) Submarine erosional troughs in the northern South China Sea: Evidence for Early Miocene deepwater circulation and paleoceanographic change. *Marine and Petroleum Geology*, **77**, 75–91.

Sun, Q., **Cartwright, J.**, **Xie, X.**, **Lu, X.**, **Yuan, S.** and **Chen, C.** (2018) Reconstruction of repeated Quaternary slope failures in the northern South China Sea. *Marine Geology*, **401**, 17–35.

ten Brink, U.S., **Barkan, R.**, **Andrews, B.D.** and **Chaytor, J.D.** (2009) Size distributions and failure initiation of submarine and subaerial landslides. *Earth and Planetary Science Letters*, **287**, 31–42.

Thiéblemont, A., **Hernández-Molina, F.J.**, **Miramontes, E.**, **Raisson, F.** and **Penven, P.** (2019) Contourite depositional systems along the Mozambique channel: The interplay between bottom currents and sedimentary processes. *Deep Sea Research Part I: Oceanographic Research Papers*, **147**, 79–99.

Tian, J., **Yang, Q.**, **Liang, X.**, **Xie, L.**, **Hu, D.**, **Wang, F.** and **Qu, T.** (2006) Observation of Luzon Strait transport. *Geophys. Res. Lett.*, **33**, L19607.

Uenzelmann-Neben, G., **Weber, T.**, **Grützner, J.** and **Thomas, M.** (2017) Transition from the Cretaceous ocean to Cenozoic circulation in the western South Atlantic — A twofold reconstruction. *Tectonophysics*, **716**, 225–240.

Van Rooij, D., **Iglesias, J.**, **Hernández-Molina, F.J.**, **Ercilla, G.**, **Gomez-Ballesteros, M.**, **Casas, D.**, **Llave, E.**, **De Hauwere, A.**, **Garcia-Gil, S.**, **Acosta, J.** and **Henriet, J.-P.** (2010) The Le Danois Contourite Depositional System: Interactions between the Mediterranean Outflow Water and the upper Cantabrian slope (North Iberian margin). *Marine Geology*, **274**, 1–20.

Vandorpe, T., **Martins, I.**, **Vitorino, J.**, **Hebbeln, D.**, **García, M.** and **Van Rooij, D.** (2016) Bottom currents and their influence on the sedimentation pattern in the El Arraiche mud volcano province, southern Gulf of Cadiz. *Marine Geology*, **378**, 114–126.

Vandorpe, T., **Van Rooij, D.** and **De Haas, H.** (2014) Stratigraphy and paleoceanography of a topography-controlled contourite drift in the Pen Duick area, southern Gulf of Cádiz. *Marine Geology*, **349**, 136–151.

Verdicchio, G. and **Trincardi, F.** (2008) Mediterranean shelf-edge muddy contourites: examples from the Gela and South Adriatic basins. *Geo-Mar Lett*, **28**, 137–151.

Viana, A.R., **Hercos, C.M.**, **De Almeida, W.**, **Magalhães, J.L.** and **De Andrade, S.B.** (2002) Evidence of bottom current influence on the Neogene to Quaternary sedimentation along the northern Campos Slope, SW Atlantic Margin. *Memoirs*, **22**, 249–259.

Wang, X., **Wang, Y.**, **He, M.**, **Chen, W.**, **Zhuo, H.**, **Gao, S.**, **Wang, M.** and **Zhou, J.** (2017) Genesis and evolution of the mass transport deposits in the middle segment of the Pearl River canyon, South China Sea: Insights from 3D seismic data. *Marine and Petroleum Geology*, **88**, 555–574.

Wang, X., **Wang, Y.**, **Tan, M.** and **Cai, F.** (2020) Deep-water deposition in response to sea-level fluctuations in the past 30 kyr on the northern margin of the South China Sea. *Deep Sea Research Part I: Oceanographic Research Papers*, **163**, 103317.

Wang, X., **Zhuo, H.**, **Wang, Y.**, **Mao, P.**, **He, M.**, **Chen, W.**, **Zhou, J.**, **Gao, S.** and **Wang, M.** (2018) Controls of contour currents on intra-canyon mixed sedimentary processes: Insights from the Pearl River Canyon, northern South China Sea. *Marine Geology*, **406**, 193–213.

Wilckens, H., **Schwenk, T.**, **Lüdmann, T.**, **Betzler, C.**, **Zhang, W.**, **Chen, J.**, **Hernández-Molina, F.J.**, **Lefebvre, A.**, **Cattaneo, A.**, **Spieß, V.** and **Miramontes, E.** (2023) Factors controlling the morphology and internal sediment architecture of moats and their associated contourite drifts. *Sedimentology*, **70**, 1472–1495.

Yang, Q., **Tian, J.** and **Zhao, W.** (2010) Observation of Luzon Strait transport in summer 2007. *Deep Sea Research Part I: Oceanographic Research Papers*, **57**, 670–676.

Yang, Y., **Yang, J.**, **Li, W.** and **Jing, S.** (2024) Slope instability and submarine-moat initiation: Insights from the northern South China sea margin. *Marine and Petroleum Geology*, **160**, 106610.

Yin, S., **Hernández-Molina, F.J.**, **Zhang, W.**, **Li, J.**, **Wang, L.**, **Ding, W.** and **Ding, W.** (2019) The influence of oceanographic processes on contourite features: A multidisciplinary study of the northern South China Sea. *Marine Geology*, **415**, 105967.

Yu, X., **Wang, J.**, **Liang, J.**, **Li, S.**, **Zeng, X.** and **Li, W.** (2014) Depositional characteristics and accumulation model of gas hydrates in northern South China Sea. *Marine and Petroleum Geology*, **56**, 74–86.

Zhang, W., **Hanebuth, T.J.J.** and **Stöber, U.** (2016) Short-term sediment dynamics on a meso-scale contourite drift (off NW Iberia): Impacts of multi-scale oceanographic processes deduced from the analysis of mooring data and numerical modelling. *Marine Geology*, **378**, 81–100.

Zhao, Y., **Liu, Z.**, **Zhang, Y.**, **Zhang, X.**, **Ma, P.**, **Yu, X.**, **Ling, C.**, **Lin, B.** and **Zhang, J.** (2024) Formation mechanism of drift-moat contourite systems revealed by in-situ observations in the South China Sea. *Earth and Planetary Science Letters*, **628**, 118585.

Zhou, W., **Wang, Y.**, **Gao, X.**, **Zhu, W.**, **Xu, Q.**, **Xu, S.**, **Cao, J.** and **Wu, J.** (2015) Architecture, evolution history and controlling factors of the Baiyun submarine canyon system from the middle Miocene to Quaternary in the Pearl River Mouth Basin, northern South China Sea. *Marine and Petroleum Geology*, **67**, 389–407.

Zhu, C., **Cheng, S.**, **Li, Q.**, **Shan, H.**, **Lu, J.**, **Shen, Z.**, **Liu, X.** and **Jia, Y.** (2019) Giant Submarine Landslide in the South China Sea: Evidence, Causes, and Implications. *JMSE*, **7**, 152.

Zhu, M., **Graham, S.**, **Pang, X.** and **McHargue, T.** (2010) Characteristics of migrating submarine canyons from the middle Miocene to present: Implications for paleoceanographic circulation, northern South China Sea. *Marine and Petroleum Geology*, **27**, 307–319.

FIGURE CAPTIONS

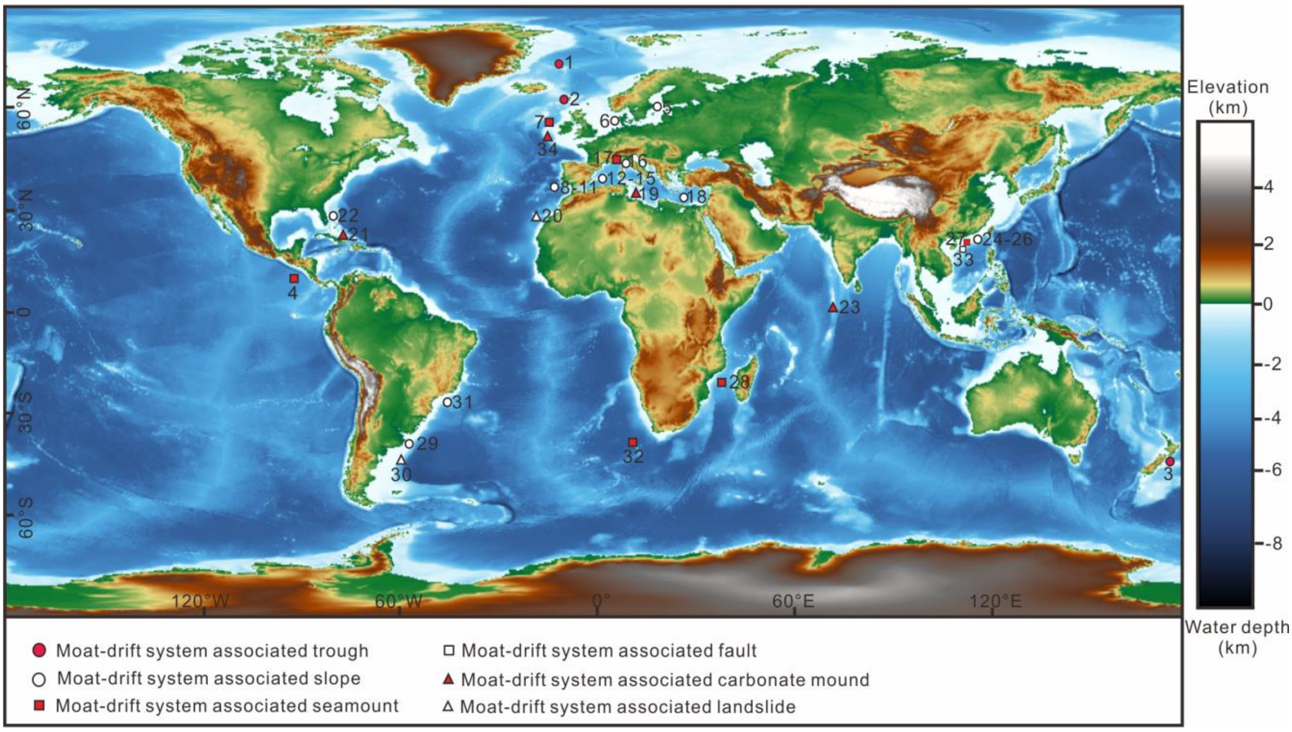

Fig. 1 Global distribution map of moat-drift contourite systems on continental margins. A list of supplementary materials can be found in the appendix Table S1.

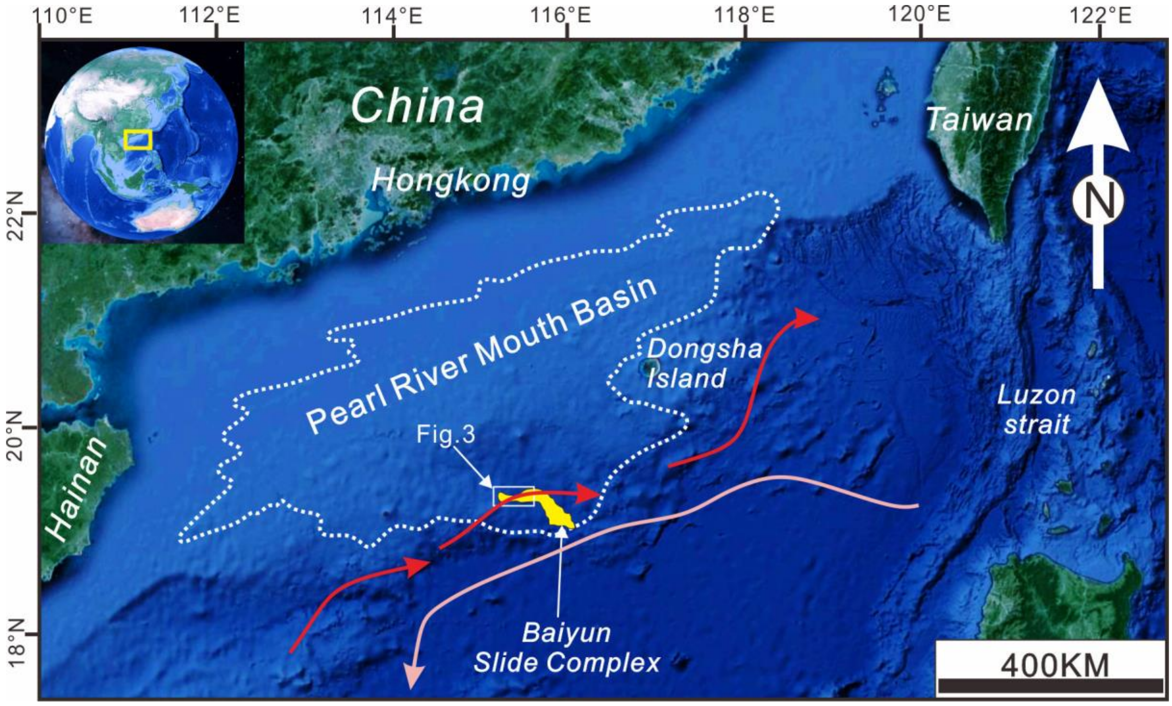

Fig. 2 Geographic and oceanographic contexts of the northern continental margin of the South China Sea. The white dotted line denotes the position of the Pearl River Mouth Basin. The paths of intermediate- deep-water masses flowing along the northern South China Sea are respectively indicated by red and orange arrows. The Baiyun Slide is marked in yellow. The white box represents the specific location of the study area, as also shown in Fig. 3.

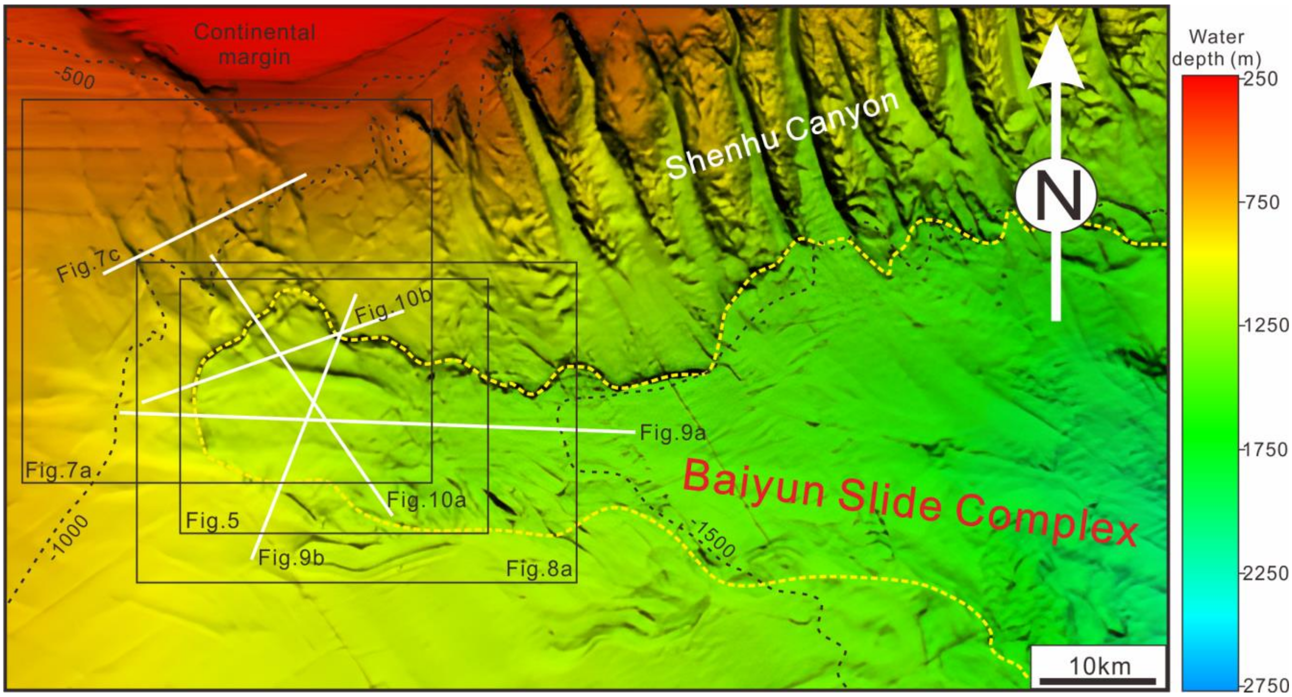

Fig. 3 Multibeam bathymetric map highlighting main bathymetric features in the study area. Bathymetric contours are shown as black dashed lines with a spacing of 500 m. The white solid lines reveal the location of the seismic profiles interpreted in this work. In addition, the yellow dashed line follows the boundary of the Baiyun Slide.

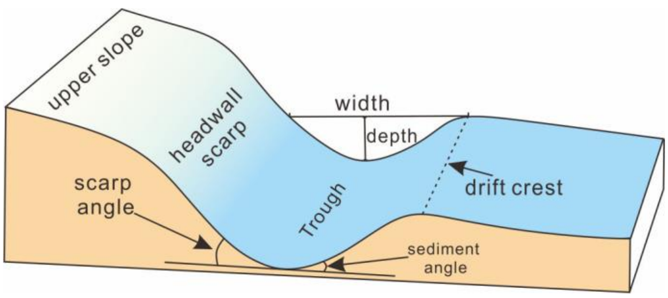

Fig. 4 Sketch illustrating the geomorphic parameters measured near the trough. Figure is modified from Wilckens et al. (2023).

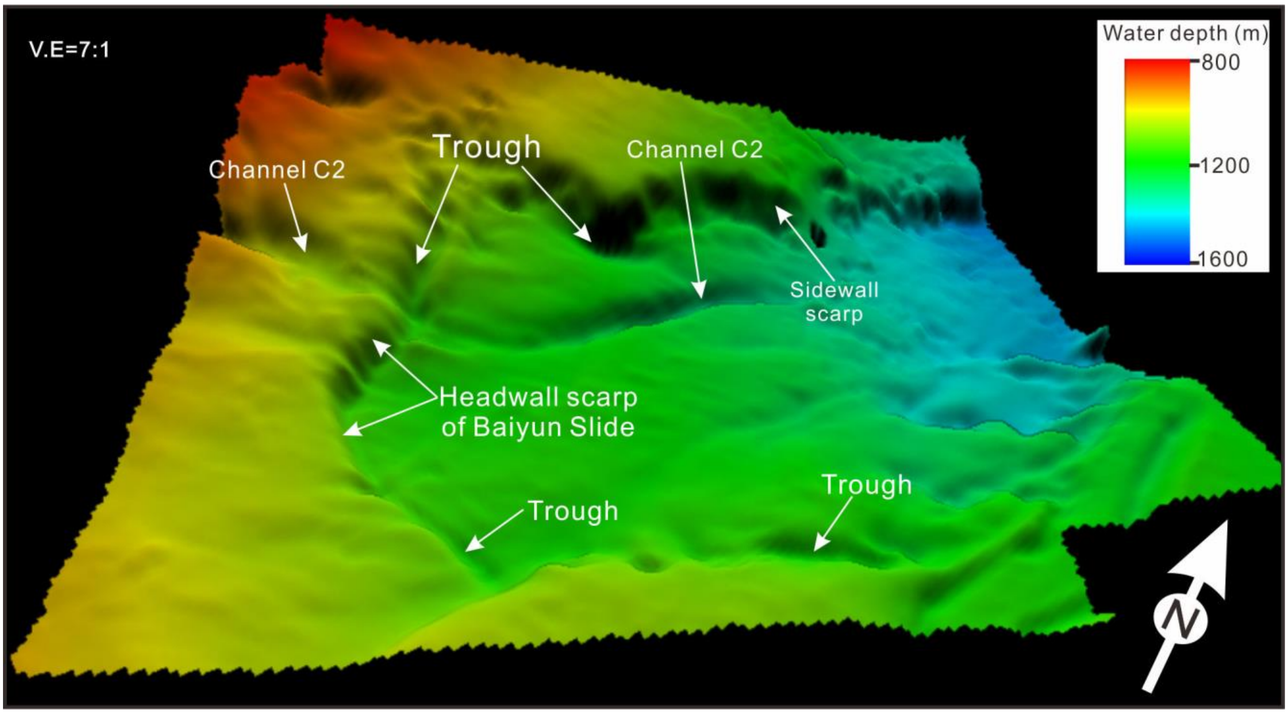

Fig. 5 Three-dimensional view of the high-resolution bathymetric data interpreted in this work. The figure shows the detailed seafloor morphology near the trough and the Baiyun Slide's headwall and lateral scarps (refer to Fig. 3 for location).

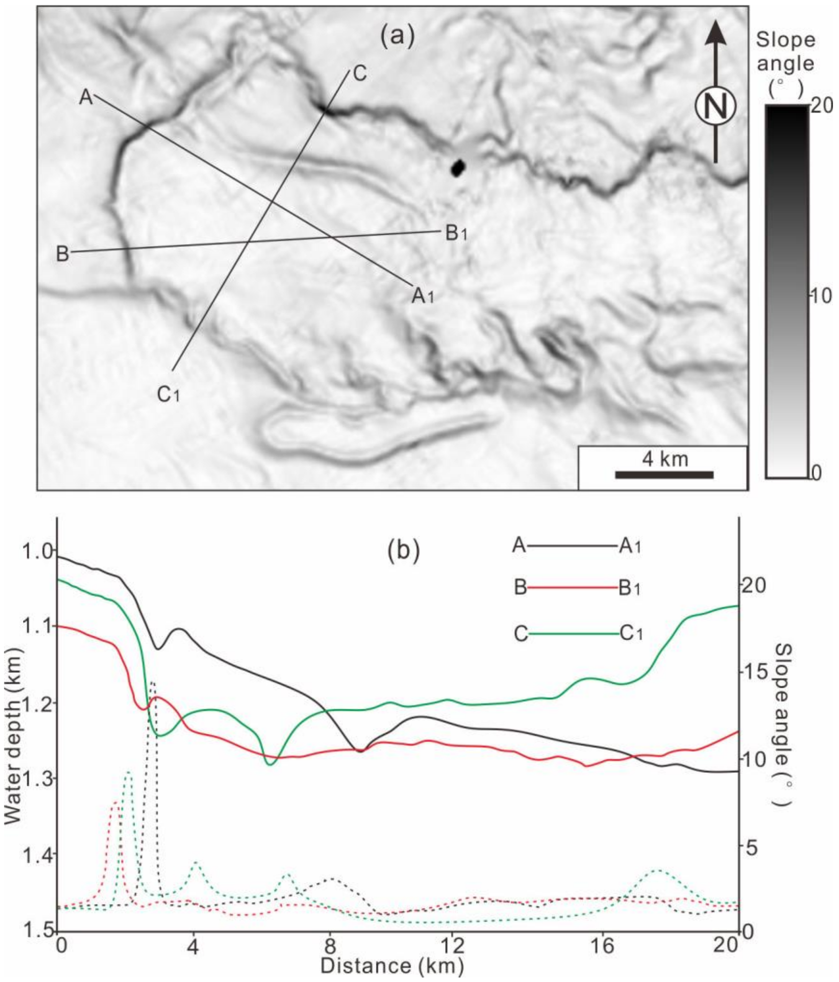

Fig.6 (a) Slope map highlighting the variations in the angle of the headwall region of the Baiyun Slide. The black solid lines refer to the cross-sections shown in Fig. 6b. (b) Solid lines represent bathymetric profiles characterizing the morphology of the study area at three distinct locations. Dashed lines indicate the variations in slope angles within the study area. The locations of the profiles are shown in Fig. 6a.

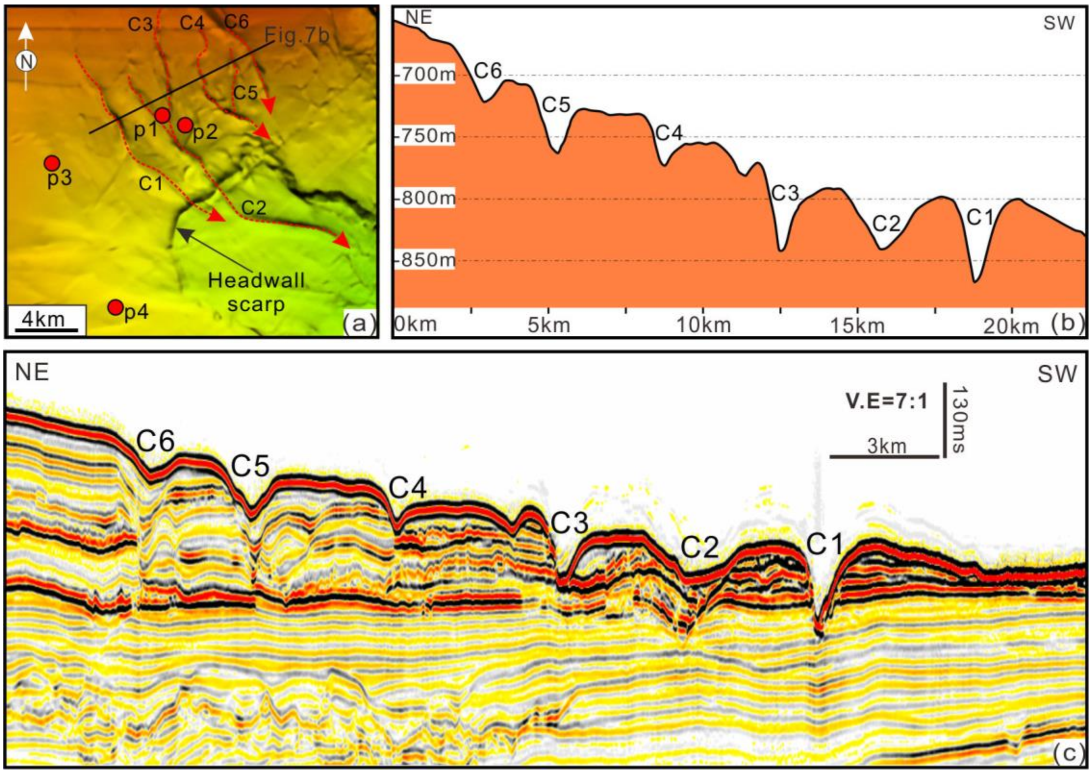

Fig. 7 (a) Multibeam bathymetric map showing the downslope-oriented channels C1 to C6 in the headwall region of the Baiyun Slide Complex. Please see the location in Fig. 3. (b) Bathymetric profile illustrating the detailed seafloor morphology of the downslope-oriented channels C1 to C6. See location in Fig. 7a. (c) Seismic profile revealing the internal architecture of these channels within the headwall region. See location of the seismic profile in Fig. 3.

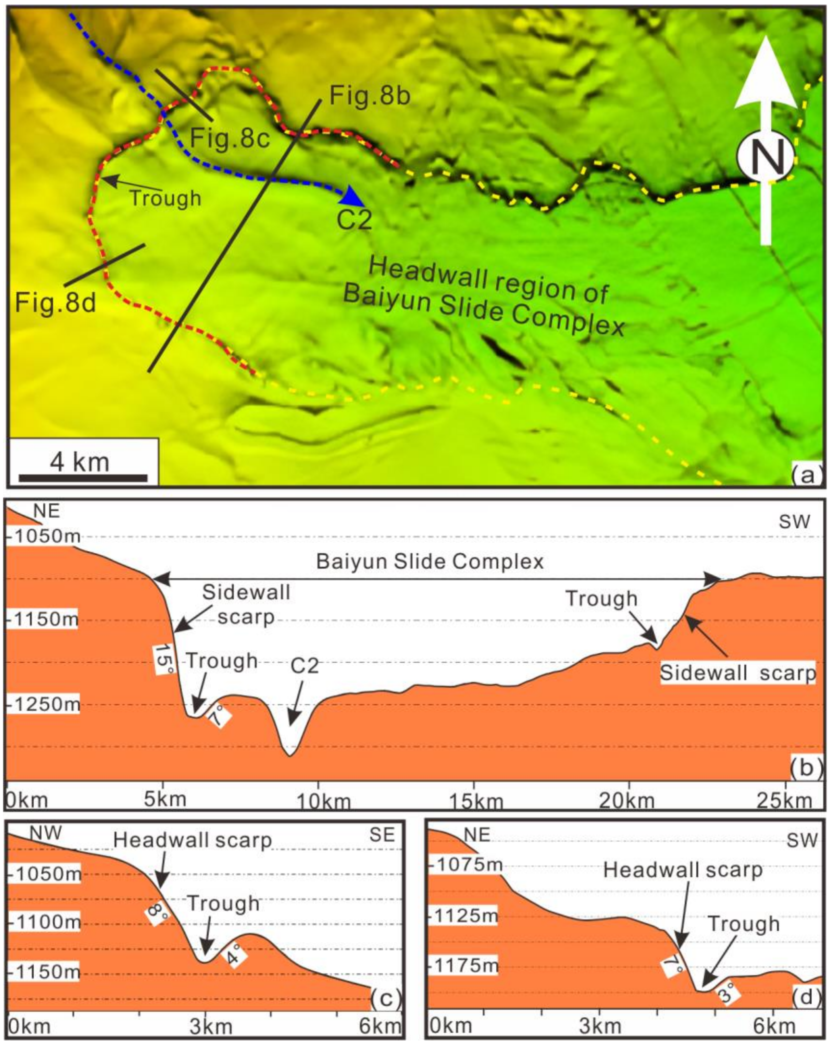

Fig. 8 (a) Enlarged multibeam bathymetric map providing seafloor morphometric data for the headwall region of the Baiyun Slide. The red dashed line highlights the development of a trough along the landslide scarps, while the solid black lines show the position of bathymetric profiles in (b), (c) and (d). (b)-(d) Bathymetric profiles across the scarps of the Baiyun Slide further confirm the presence of a trough in the study area.

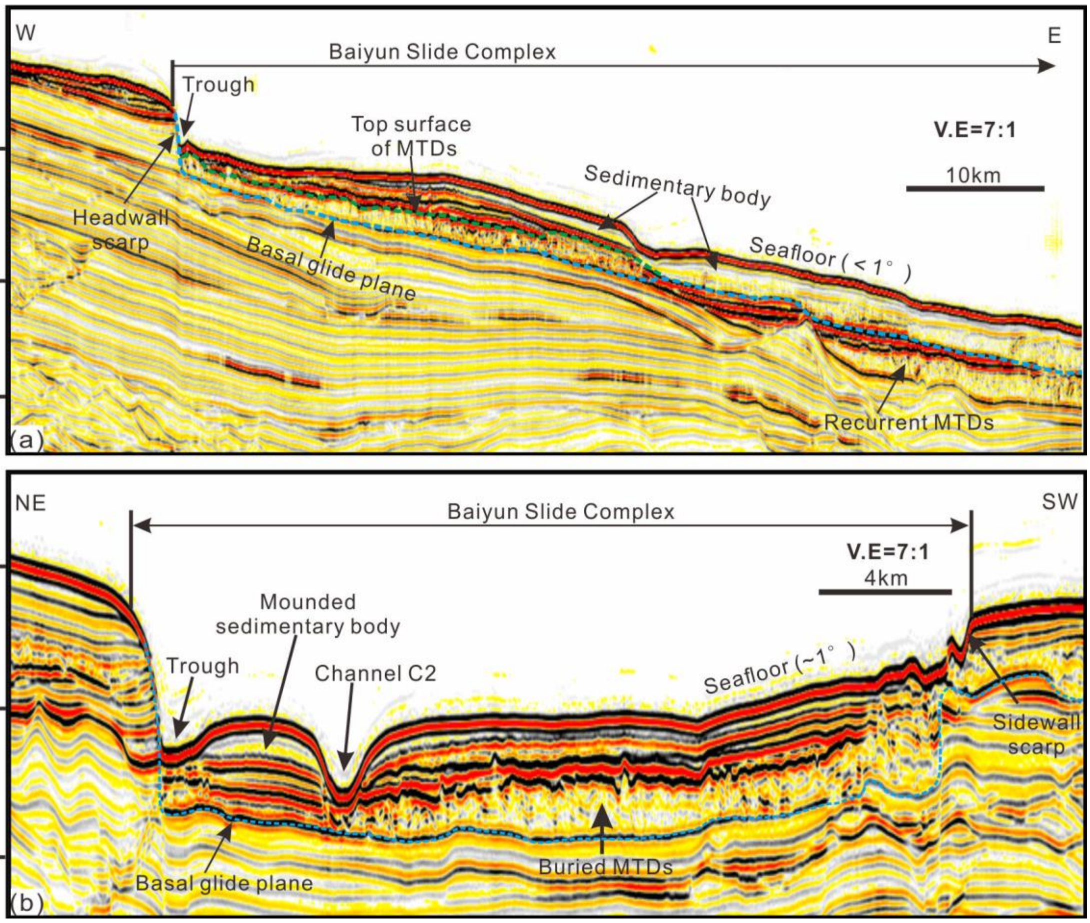

Fig. 9 (a) Seismic profiles imaging the headwall and interior region of the Baiyun Slide. The profiles highlight the morphology of landslide scarps and the associated MTDs. (b) Seismic profile across the sidewall of the Baiyun Slide revealing the presence of the trough, mounded sedimentary body, and buried MTDs.

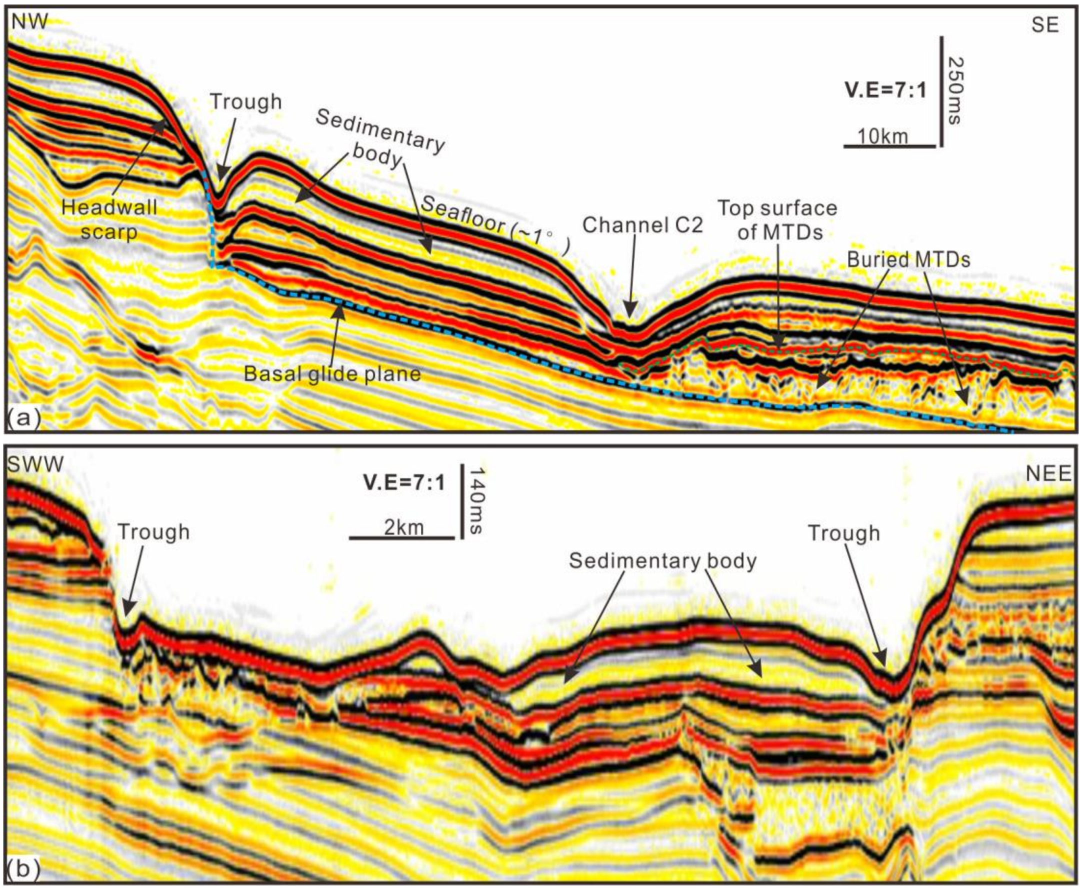

Fig. 10 (a) 3D seismic profile across the northern section of the Baiyun Slide's headwall region revealing variations in the thickness of sedimentary body. The profile reveals the presence of a trough along the headwall scarp, as well as buried MTDs in the slide. (b) 3D seismic profile imaging the trough close to the headwall and sidewall scarps of the Baiyun Slide.

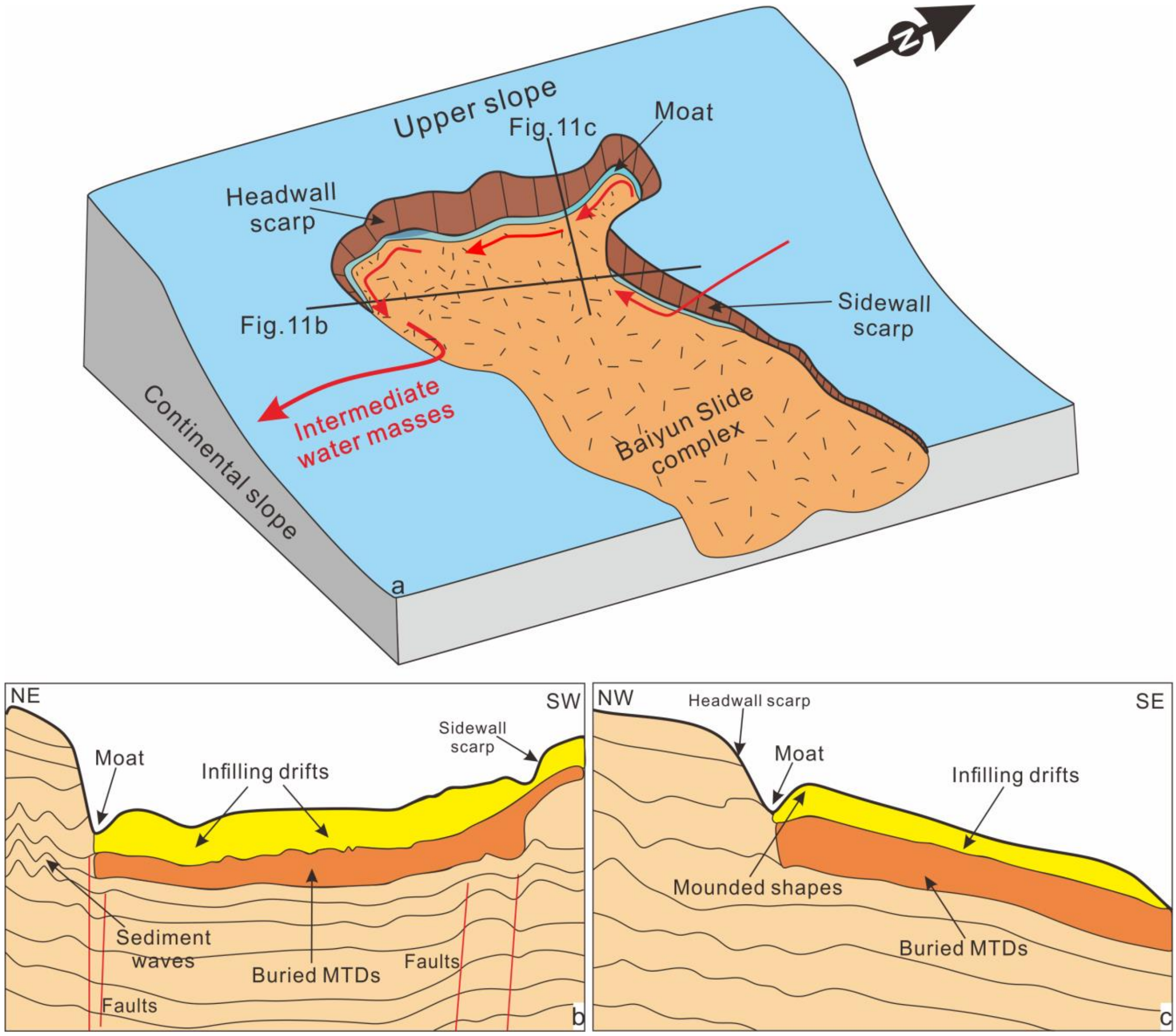

Fig. 11 Conceptual model summarizing the evolution of the study area. (a) The Baiyun Slide mobilized a substantial volume of sediment resulting in the formation of steep landslide scarps. As a result, the flow of bottom currents branched and followed the contours as they entered the headwall region. (b)-(c) The presence of landslide scarps enhanced bottom flow velocities in its vicinity, leading to sediment erosion and the initiation of a moat. Simultaneously, the intensified bottom flow processes resuspend and redistribute sediments, causing them to settle and build mounded features at one side of this same moat. In areas with unchanged bottom-current velocities, suspended particles gradually settle out over time resulting in the formation of infilling drifts.

SUPPLEMENTARY MATERIAL

Table S1 Summary of modern moat-drift contourite systems documented worldwide.

Number	Reference	Study area	Moat-drift system location
1	Rebesco et al. 2016	NW Barents Sea	Trough
2	Masson et al. 2002	North Rockall Trough	Trough
3	Lewis andd Pantin. 2002	Hikurangi Trough	Trough
4	Clarke et al. 2018	Southwest Costa Rica	Seamount
5	Sivkov et al. 2002	Baltic Sea	Slope
6	Liu et al. 2020	Gulf of Biscay	Slope
7	Howe et al. 2006	Rosemary Bank seamount	Seamount
8	Hernández-Molina et al. 2016	Gulf of Cadiz	Slope
9	García et al. 2009	Gulf of Cadiz	Slope
10	Vandorpe et al. 2014	Gulf of Cadiz	Slope
11	Van Rooij et al. 2010	Gulf of Cadiz	Slope
12	Verdicchio and Trincardi 2006	Adriatic Sea	Slope
13	Martorelli et al. 2010	Adriatic Sea	Slope
14	Miramontes et al. 2019	Balearic Sea	Slope
15	Miramontes et al. 2016	Tyrrhenian Sea	Slope
16	Ercilla et al. 2016	Alboran Sea	Slope
17	Palomino et al. 2011	Alboran Sea	Seamount
18	Tripsanas et al. 2016	Aegean Sea	Slope
19	Micallef et al. 2016	Mediterranean Sea	Carbonate mound
20	Acosta et al. 2005	Canary Islands	Submarine landslide
21	Lüdmann et al. 2016	Santaren Channel	Carbonate mound
22	Mulder et al. 2019	Santaren Channel	Slope
23	Betzler et al. 2013	North Indian Ocean	Carbonate mound
24	Yin et al. 2019	South China Sea	Slope
25	Zhao et al. 2015	South China Sea	Slope
26	Palamenghi et al. 2015	South China Sea	Slope
27	Chen et al. 2014	Northwest South China Sea	Seamount
28	Miramontes et al. 2021	Mozambique Channel	Seamount
29	Wilckens et al. 2021	South Atlantic	Slope

30	Uenzelmann-neben et al. 2017	South Atlantic	Submarine landslide
31	Alves et al., 2011	Offshore Brazil	Slope
32	Gruetzner et al. 2016	Agulhas Ridge	Seamount
33	Liu et al., 2021	Southern South China Sea	Fault
34	Hovland et al., 1994	Western Ireland	Carbonate mound